INDIAN JOURNAL OF SCIENCE AND TECHNOLOGY

RESEARCH ARTICLE

Characterization of a Novel System of Bismuth Lead Borosilicate Glass Containing Copper

Madabushanam Gopi Krishna[1], Ravi Kumar Guntu[2]*, Md Shareefuddin[1], N V Prasad[1]

1 Department of Physics, Osmania University, Hyderabad, 500 007, Telangana, India
2 Department of Physics, Sreenidhi Institute of Science and Technology, JNT University, Hyderabad, 501 301, Telangana, India

OPEN ACCESS

Received: 11-01-2024

Accepted: 22-01-2024

Published: 22-02-2024

Citation: Krishna MG, Guntu RK, Shareefuddin M, Prasad NV (2024) Characterization of a Novel System of Bismuth Lead Borosilicate Glass Containing Copper. Indian Journal of Science and Technology 17(9): 819-829. https://doi.org/10.17485/IJST/v17i9.81

* **Corresponding author**.

drgrk1985@gmail.com

Funding: None

Competing Interests: None

Published By Indian Society for Education and Environment (iSee)

ISSN
Print: 0974-6846
Electronic: 0974-5645

Abstract

Objectives: The primary objective of the present investigation was to examine the impact of Bi^{3+} ions on the optical, radiation shielding, dielectric and structural characteristics of lead borosilicate glasses doped with CuO. **Method:** In this view, we planned to utilize the conventional rapid melt quenching method to produce glasses with the following chemical composition: 25 PbO + 15 B_2O_3 + 0.1 CuO + (59.9-x) SiO_2:x Bi_2O_3($0 \leq x \leq 12$). **Findings:** The samples' non-crystalline characteristics were validated through XRD and SEM analysis, respectively, while their glass-forming capabilities were assessed through DTA studies. Utilizing the FT–IR and Raman analyses, the numerous structural units were determined. According to the findings of the FT-IR, and Raman analyses, the degree of disorder in the glass network increased. By means of optical absorption experiments, the optical properties of glasses were determined. The results obtained from optical absorption spectral investigations indicated that the concentration of octahedral Cu^{2+} ions increased gradually as the Bi_2O_3 concentration increased to 12 mol %. The dielectric properties of the glasses, suggested that the dielectric constant values of glasses containing Bi_2O_3 in concentrations below 12 mol% increase gradually. Additionally, the radiation shielding properties of the glasses are investigated. The values of radiation protection ability found to be purely function of Bi_2O_3 concentration. **Novelty:** The results suggest that the glasses' thermal stability, dielectric constant, optical band gap and radiation shielding ability values purely function of Bi_2O_3 concentration.

Keywords: Borosilicate glasses; Thermal stability; Optical absorption; Radiation shielding properties; Dielectricsq

1 Introduction

Similar to borotelluride or borophosphate glasses, multicomponent borosilicate glasses exhibit durability when subjected to similar circumstances. In general, the surface contamination resistance is the main feature of borosilicate glasses [(1)]. A thin layer of

condensation forms from the water vapor on the borosilicate glass, which does not obstruct the clarity of light passing through the glass [2]. When compared to numerous other mixed glass former glasses, borosilicate glasses containing various metal cations have exceptionally extensive network forming units. Compared to ultra-silicate glasses of equivalent composition, those composed of borosilicate and lead and bismuth heavy metal ions exhibit considerably greater stability and durability [3]. Lead borosilicate glass systems are among the most suitable for forming mixed glass networks due to their extremely nonlinear compositional dependencies on glass transition temperature and ionic conductivity. In addition to serving as electrolytes in solid electrochemical cells, lead borosilicate glasses are also utilized in vacuum energy storage safety devices [4]. Recently, there has been a significant focus among researchers on the advancement of crystalline or amorphous solid electrolyte materials that exhibit exceptional electrical properties. As a result, glasses composed of lead borosilicate have been recognized as electrolyte materials with exceptional efficiency [5]. Under PbO's substantial band gap, glasses containing it exhibit exceptional transparency, even in the ultraviolet (UV) spectrum, thereby enhancing their resistance to moisture. By incorporating heavy metal oxides such as Bi_2O_3 into lead borosilicate glasses, one can impart them with distinct properties including elevated density, refractive index, dielectric constant, NIR transmission with favorable photothermal characteristics, and reduced phonon losses [6,7]. The incorporation of various transition metal ions, including Cr, Cu, and Ti, significantly enhances the properties of lead borosilicate glasses. Glasses containing Cu^{2+} are viable candidates for Q-switching circuits and non-linear optical absorbers for assisting passive laser beam variations [8]. Lead borophosphate glass systems doped with different transition metal oxides are one of the most suitable mixed glass network formers, which exhibit strong non-linear compositional dependence of space charge polarization and mass attenuation coefficient for various types of irradiations. Because of these reasons lead borosilicate glasses have significant applications such as electrolytes in solid electrochemical cells, vacuum, energy storage, radiation protection materials etc. [9].

1.1 Research Gap

The cupper ions with the $3d^9$ configuration are primarily found in the divalent state Cu^{2+}, where they can occupy a tetrahedral or octahedral occupancy depending on the glass's environment. The composition at normal temperature and pressure is the sole determinant of their capacity to modify or generate glass. It is hypothesized that the dual occupancy is because of the minor disparity in ligand field stabilization energy between the two potential coordination states of Cu^{2+} ions. These glasses may find use in the industrial sector as structural tracers in glasses, carbon monoxide sensors, and catalysts for the reduction of carbon monoxide [10]. We have investigated the effects of copper ions on the structural, optical, and dielectric characteristics of Bi_2O_3 doped lead borosilicate glasses in this study using characterization techniques as XRD, SEM, EDS, DTA, FT–IR, Raman, optical absorption, radiation shielding, and dielectric dispersion studies.

2 Methodology

For this investigation, the chemical composition of 25 PbO + 15 B_2O_3 + 0.1 CuO + (59.9-x) SiO_2:x Bi_2O_3 has been selected. Table 1 contains the complete composition. The precise concentrations of the analytic grades of PbO, Bi_2O_3, Boric acid (H_3BO_3), SiO_2, and CuO chemicals (all expressed in mole percent) were carefully mixed in an agate mortar and then liquefied in a densely walled crucible in an automatic temperature furnace for about 30 minutes, or until a transparent liquid without of voids created.

Table 1. Chemical composition of 25 PbO + 15 B_2O_3 + 0.1 CuO + (59.9-x) SiO_2 :x Bi_2O_3 glass materials

Glass	PbO (mol%)	B_2O_3 (mol%)	CuO (mol%)	SiO_2 (mol%)	Bi_2O_3 (mol%)
CuBi-0	25	15	0.1	59.9	0
CuBi-3	25	15	0.1	56.9	3
CuBi-5	25	15	0.1	54.9	5
CuBi-8	25	15	0.1	51.9	8
CuBi-10	25	15	0.1	49.9	10
CuBi-12	25	15	0.1	47.9	12

The final mixture was poured into a brass mold around at 1345 to 1350 °C, which was subsequently annealed gradually at 250 °C in a muffle furnace. Utilizing a Scale Tech digital weighing balance, the mass of the prepared containers was measured with a precision of 10^{-4} grams. The O-xylene liquid and the Archimedes method were employed to determine the densities (± 0.0001 g/cm^3) of the glass samples that were produced. After reducing the samples to the specified dimensions of 1x 1 x 0.2 cm^3, they were appropriately polished. To validate the non-crystalline characteristics of the fabricated glasses, X-ray diffraction traces

were captured utilizing a PAN analytical instrument equipped with X'Pert^3 Powder. Sample surface morphology as captured by the Hitachi S-3700N Spectrometer. The DTG – 60H (SHIMADZU) was utilized to conduct differential thermal analysis on the prepared samples. The instrument operated at a heating rate of 5.0 °C per minute, covering a temperature range of 27 to 1400 °C. The produced glasses were subjected to optical absorption investigations at room temperature using an Agilent Technologies Carry 5000 UV to NIR Region instrument with a 0.1 nm resolution within the 200 – 2200 nm wavelength range. The spectral measurements in the FT-IR range of 400-4000 cm^{-1} were acquired using a Perkin Elmer Spectrum Two instrument with four scans. Raman spectral measurements were acquired utilizing a Horrible Jobin Yvon Germany, LASER (633 nm), 20-2000 nm instrument, 100x objective lens. Utilizing Phy-x and PSD software to obtain radiation shielding measurements. The Auto lab Impudence analyzer was utilized to conduct dielectric measurements across a frequency range of 1 kHz to 1 MHz.

3 Results and Discussion

The photograph of the prepared 25 PbO + 15 B_2O_3 + 0.1 CuO + (59.9-x) SiO_2 :x Bi_2O_3 glasses is in a shown Figure 1**(a)**. The test glasses' X-ray diffraction patterns are reported in Figure 1**(b)**, which reveal no crystalline peaks in the X-ray diffraction results[11]. With respect to XRD intensities, the CuBi-12 glass was noticed highest in diffraction intensities. As per earlier research, the maximum diffraction intensities of test samples might be attributed to the closest structural compactness, least distance between atoms, highest density, and least molar volume. The chemical composition of the CuBi-12 glass verified using energy dispersion spectra. Which signifies the chemicals such as oxygen, bismuth, lead, copper boron and silicon with in the glass. Which also reveal 25 mol% of PbO, 15 mol% of B_2O_3, 0.1 mol% of CuO, 47.9 mol% of SiO_2 and 12 mol% of Bi_2O_3 with atomic weight % of glass. All these results of the CuBi-12 glass chemical analysis represented in Figure 1 **(c)**. The surface morphology of the 25 PbO + 15 B_2O_3 + 0.1 CuO + (59.9-x) SiO_2 :x Bi_2O_3test samples recorded, which are observed to have no crystalline behavior. At 10, 20, 5 0 and 100 mm range, one of the tests CuBi-12 glass morphological reports of test glasses represented in Figure 2 which is suggesting glassy behavior.

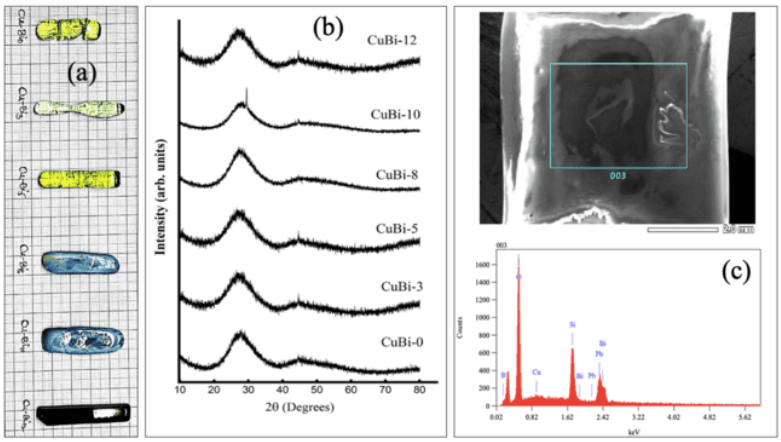

Fig 1. (a) The photograph, (b) XRD patterns, and (c) Chemical analysis of the CuBi-12 glass of 25 PbO + 15 B_2O_3 + 0.1 CuO + (59.9-x) SiO_2 : x Bi_2O_3 glasses

The physical properties of 25 PbO + 15 B_2O_3 + 0.1 CuO + (59.9-x) SiO_2 :x Bi_2O_3glasses reported in Table 2. For the prepared glasses, as the concentration of Bi_2O_3 increases, the density depends and an increase in average molecular weight is observed. As the concentration of CuO increases, the anticipated ionic concentration, field strength, and molar volume increase. Whereas the associated ionic radius and polaron radius decrease[12]

It was discovered that the glass transition temperature of the 25 PbO + 15 B_2O_3 + 0.1 CuO + (59.9-x) SiO_2 :x Bi_2O_3 glasses was 420 °C, and that the value of T_g increased as the concentration of Bi_2O_3 increased. The value of the exothermic peak, which is seen at the glass crystallization temperature (T_c) of roughly 850 °C, rises with the concentration of Bi_2O_3[13]. The thermal stability {(Tc-T_g)/T_g} of glass was assessed using T_g and T_c of the glasses sample.

The usual vibrational bands of borate groups, silicate groups, PbO, Bi_2O_3, and CuO structural units are displayed in the FT-IR spectra of 25 PbO + 15 B_2O_3 + 0.1 CuO+ (59.9-x) SiO_2 : x Bi_2O_3 glasses, as provided in Table 4 and illustrated in Figure 4. SiO_2 vibrational modes, including symmetrical and asymmetrical Si-O-Si units, are observed at around 926–937 cm^{-1} and 762–771 cm^{-1}. Regions of 1394–1406 cm^{-1}, 926–937 cm^{-1}, and 692–709 cm^{-1}, respectively, are the bands that originate from BO_3, BO_4

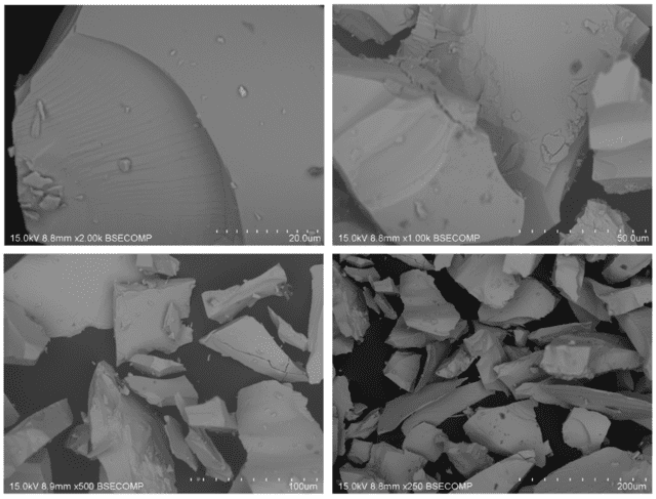

Fig 2. Surface morphology of the CuBi-12 glass at 10, 20, 50 and 100 mm range

Table 2. Physical properties of 25 PbO + 15 B_2O_3 + 0.1 CuO + (59.9-x) SiO_2 :x Bi_2O_3 glasses measures at room temperature

Glass	CuBi-0	CuBi-3	CuBi-5	CuBi-8	CuBi-10	CuBi-12
ρ(gm/cm^3)	4.49	4.56	4.74	4.87	5.14	5.37
Ni(x10^{20})	-	2.07	2.28	2.33	2.41	2.51
ri(Å)	-	0.169	0.166	0.164	0.162	0.159
rp(Å)	-	6.75	6.60	6.52	6.45	6.18
Vm(cm^{3}mol^{-1})	30.467	29.104	28.793	27.669	25.842	22.737
Fi(x10^{14}eV cm^{-2})	-	2.15	2.23	2.3	2.41	2.45

Table 3. Summary on data of DTA studies of 25 PbO + 15 B_2O_3 + 0.1 CuO + (59.9-x) SiO_2 :x Bi_2O_3 glasses

Glass	CuBi-0	CuBi-3	CuBi-5	CuBi-8	CuBi-10	CuBi-12
T_g(°C)	585	586	587	589	591	594
Thermal stability	0.659	0.670	0.679	0.689	0.696	0.702

units, and B–O–B connections. The Pb–O–Pb symmetric units were observed at 692 - 709 cm^{-1} in the vicinity, respectively. In the ranges, 606 – 612 cm^{-1} and 434 – 446 cm^{-1}, respectively, the BiO_4 tetrahedral and BiO_6 octahedral vibrations were observed. Within the range of 694–709 cm^{-1}, the bands resulting from Cu–O specific vibrations will be predicted [14,15].

Table 4. Data on infrared spectra of 25 PbO + 15 B

Glass	CuBi-0	CuBi-3	CuBi-5	CuBi-8	CuBi-10	CuBi-12
BO_3units (cm^{-1})	1401	1398	1396	1395	1392	1391
Si-O-Si asymmetrical (cm^{-1})	1022	1020	1016	1012	1006	998
Si-O-Si symmetrical (cm^{-1})	760	765	772	776	780	784
BO_4 units(cm^{-1})	910	911	913	915	917	920
Pb-O-Pb units (cm^{-1})	510	513	515	519	523	530
Bi-O linkages(cm^{-1})	850	852	855	857	859	860
CuO specific vibrations (cm^{-1})	580	581	585	586	588	591

As seen in Figure 5, the Raman spectra of the 25 PbO + 15 B_2O_3 + 0.1 CuO + (59.9-x) SiO_2 : x Bi_2O_3 glasses exhibit characteristic vibrational bands of PbO, Bi_2O_3, CuO, silicate groups, and borate groups. Table 5 contained the Raman band assignment. The SiO_2 vibrational modes observed at 784 – 799 cm^{-1} and 1052 – 1067 cm^{-1} include Si-O-Si bending and stretching units.

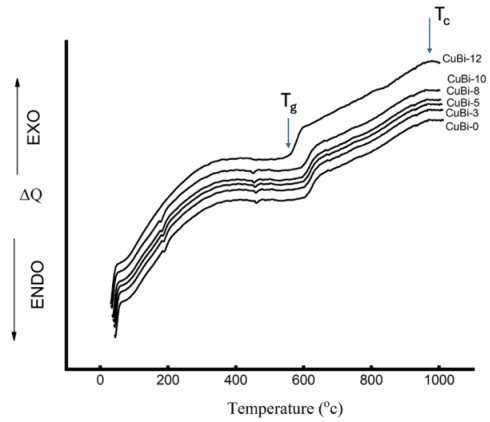

Fig 3. DTA thermograms of the 25 PbO + 15 B_2O_3 + 0.1 CuO + (59.9-x) SiO_2 :x Bi_2O_3 glasses

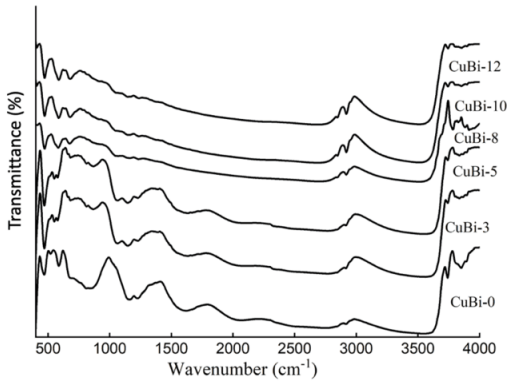

Fig 4. FT-IR spectra of 25 PbO + 15 B_2O_3 + 0.1 CuO + (59.9-x) SiO_2 :x Bi_2O_3 glasses recorded at room temperature

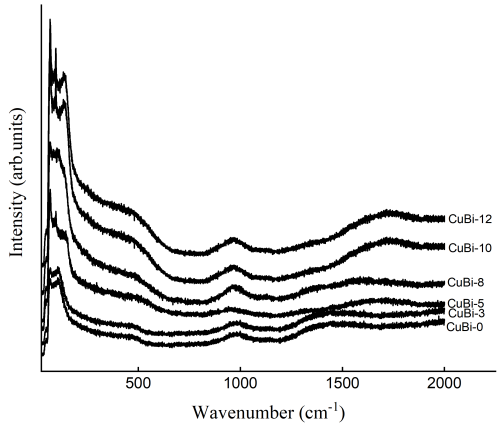

Fig 5. Raman spectra of 25 PbO + 15 B_2O_3 + 0.1 CuO + (59.9-x) SiO_2 :x Bi_2O_3 glasses recorded at room temperature

The regions 794 –776 cm^{-1}, 741 – 757 cm^{-1} and 692 – 709 cm^{-1} are home to the bands that originate from BO_3, BO4 units, and B-O-B connections, respectively. The Pb–O–Pb symmetric units were observed at 667 and 690 cm–1 in the vicinity, respectively. The areas 606 – 612 cm^{-1} and 395 – 415 cm^{-1} are where the BiO_4 tetrahedral and BiO_6 octahedral vibrations were seen, respectively. In the range of 632 – 645 cm^{-1}, the bands resulting from Cu–O specific vibrations are anticipated [16,17].

Table 5. Summary on Raman spectra of 25 PbO + 15 B_2O_3 + 0.1 CuO + (59.9-x) SiO_2 :x Bi_2O_3 glasses

Glass	CuBi-0	CuBi-3	CuBi-5	CuBi-8	CuBi-10	CuBi-12
BO_3 units (cm^{-1})	794	791	787	785	780	776
Si-O-Si bending (cm^{-1})	784	787	791	794	796	799
Si-O-Si stretching (cm^{-1})	1052	1055	1058	1061	1064	1067
BO_4 units(cm^{-1})	741	744	748	751	754	757
Pb-O units (cm^{-1})	667	670	673	677	685	690
Bi-O linkages (cm^{-1})	395	397	403	408	412	415
CuO vibrations (cm^{-1})	632	635	638	640	643	645

The optical absorption spectrum of 25 PbO + 15 B_2O_3 + 0.1 CuO + (59.9-x) SiO_2 :x Bi_2O_3 glasses, recorded at room temperature, is shown in Figure 6**(a)**. The band gap values of glasses can be found by examining the Tauc plots of glasses, as shown in Figure 6 **(b)**. In this view, the glass with the highest concentration of CuO 12 mol% among all the other glasses was noted. Table 6 presents the results of current glasses together with identifications and evaluations of the absorption spectra [18]. As the amount of Bi_2O_3 increases, the optical band gap parameter decreases, as shown by the Tauc plots and observed optical absorption spectra of the current glasses. This is because there are more non-bridging oxygens and bond defects in the glass ceramic network, which in turn lead to Cu^{2+} and Bi^{3+} ions depolymerizing the network of glass ceramics. When Bi_2O_3 is added to the glass network up to a 12 mol% concentration, CuO_6 ions rise and various donor ions develop, which tend to overlap with excited states of electrons. These many explanations show that the impurity energy band diffuses into the original band gap, causing the optical band gap to decrease [19].

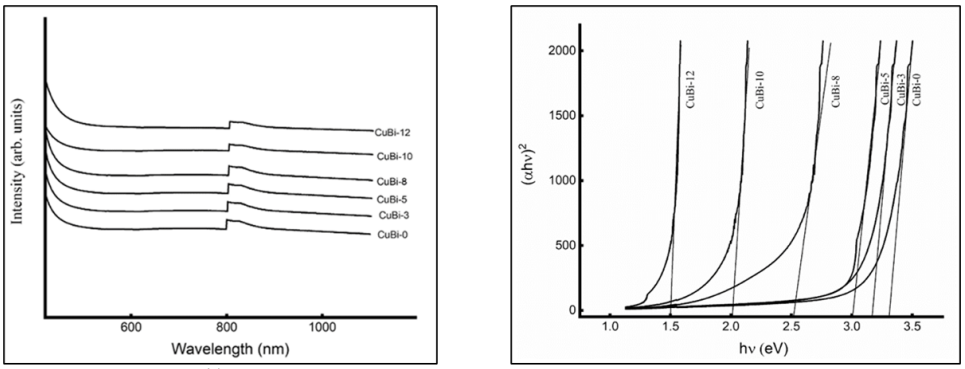

Fig 6. (a) Optical absorption spectra of 25 PbO + 15 B_2O_3 + 0.1 CuO + (59.9-x) SiO_2 :x Bi_2O_3 glasses recorded at room temperature, (b) Tauc plots of 25PbO+ 15 B_2O_3 + 0.1 CuO + (59.9-x) SiO_2 : x Bi_2O_3 glasses

Table 6. Summary on optical absorption of 25 PbO + 15 B_2O_3 + 0.1 CuO + (59.9-x) SiO_2 :x Bi_2O_3 glass materials recorded at room temperature

Glass	CuBi-0	CuBi-3	CuBi-5	CuBi-8	CuBi-10	CuBi-12
Optical band gap (eV)	3.3	3.2	3	2.5	2	1.5
Urbach Energy (eV)	0.0785	0.0781	0.0776	0.0771	0.0766	0.0762

The optical absorption spectra of the 25 PbO + 15 B_2O_3 + 0.1 CuO + (59.9-x) SiO_2 :x Bi_2O_3 glasses indicate that Cu^{2+} ions deform and occupy octahedral sites at low concentrations of Bi_2O_3. As the concentration increases up to 12 mol%, the occupancy rate increases; however, as the concentration increases, the octahedral occupancy in the glass matrix decreases. An increase of 12 mol% of Bi_2O_3 in the concentration of Bi^{3+} ions at octahedral sites in the glass system results in a greater production of NBOs and bound electrons at donor centers. Consequently, vacant third states of adjacent Cu^{2+} ion sites coincide with the excited states of the localized electrons that were initially confined in Cu^{+} sites. Consequently, the absorption edge transitions to the higher wavelength region, and the optical band gap diminishes substantially due to the widening and merging of the impurity band with the main band. The observed alterations in the absorption edge and optical band gap may be attributed to a reduction in the interaction between the p-electrons in the conductions band of silicate ions and the localized d electrons of substitutionally positioned copper ions. As network modifiers, the octahedral copper ions consequently decrease the rigidity of the produced samples. An increase in the concentration of Bi_2O_3 (> 12 mol%) in the glasses results in a reduction in the density of interrelated groups containing ions positioned interstitial and the concentration of NBOs. This phenomenon potentially signifies a decline in the number of donor centers occupied by electrons. The absorption edge inherently shifts in favor of shorter wavelengths due to the expansion of the optical band gap.

Using the Phy-X/PSD programme the shielding characteristics of the 25 PbO + 15 B_2O_3 + 0.1 CuO + (59.9-x) SiO_2 :x Bi_2O_3 glasses are examined. The half value layer characterizes how well the radiation can pass through the test glasses. Additionally, it helps with shielding design. The sample's mean free path indicates how well photons can pass through it. It is discovered that there is an increase in photon energy variation in the values of MAC[20]. The results indicate that the Cu^{2+} ions are indicated by the K-absorption edge at approximately 0.0679 MeV. The fluctuation in MAC, MFP (mean free path), HVL (half layer width), and RPE (radiation protection efficiency) with increasing incident photon energy is reported in Figure 7**(a), (b), (c),** and **(d)**. Test glasses have a higher degree of density due to the CuO_6 octahedral units. The structural units of Pb-O-Si, Bi-O-B, and Bi-O-Cu are the additional cause of the high glass density. It is possible to represent the MAC tendency versus photon energy using an exponential decaying pattern.

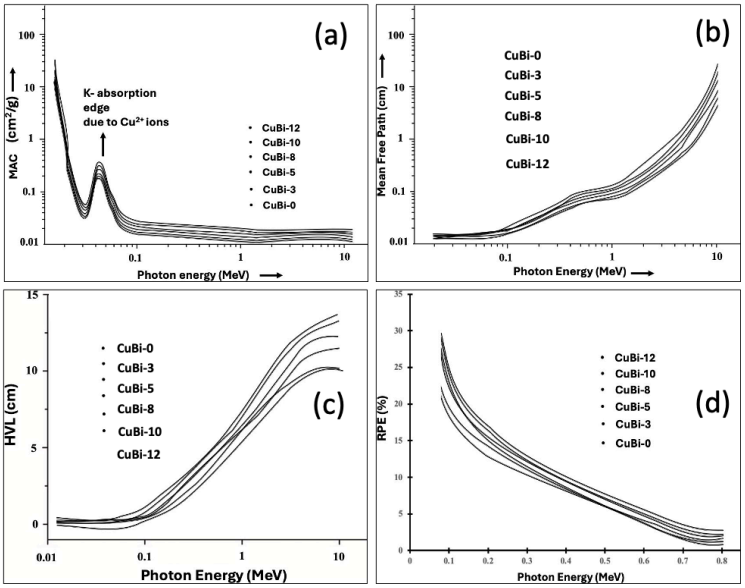

Fig 7. (a) Variation in MAC, (b) Variation in MFP, (c) Variation in HVL, and (d) Variation in RPE with Photon energy of 25 PbO + 15 B_2O_3 + 0.1 CuO + (59.9-x) SiO_2 : x Bi_2O_3 glasses

Additionally, as the content of Bi_2O_3 in the glass samples increased, the MAC values were also shown to increase. For the glasses recorded as CuBi-0 to CuBi-12, the MAC values at low energy photons E = 0.015 MeV are 17.181 and 17.371, respectively. Based on the amount of Bi_2O_3 contained in the glasses, the minimal variation in the MAC values of the test glass can be understood. The other two molecular components of the glass system, such as Bi_2O_3, PbO and B_2O_3, are maintained at an equimolar fraction in each of the manufactured glasses. The mol% of Bi_2O_3 in these glasses is increased from 0.0 to 12 mol% compared to the Bi_2O_3 concentration.

Table 7. Summary on radiation shielding properties of 25PbO + 15 B_2O_3 + 0.1 CuO + (59.9-x) SiO_2 : x Bi_2O_3 glasses recorded at room temperature

Glass	CuBi-0	CuBi-3	CuBi-5	CuBi-8	CuBi-10	CuBi-12
MAC (at 0.02 MeV)	15.245	18.245	21.225	32.345	34.545	41.045
MFP (at 10 MeV)	32	27	19	14.1	10.2	7.5
HVL (at 10 MeV)	14.22	13.75	12.85	12.62	11.45	10.21
RPE (%)	30.5	28.5	27	26	24	22

Another cause of the change in MAC values with rising Bi^{3+} ions is the NBOs during glass formation. Since the Pb^{2+}, Bi^{3+}, Si^{4+} and Cu^{2+} ions in the glasses have site symmetry, there is a greater increase in MAC values in low photon energy range. For glasses CuBi-0.0 to CuBi-2.5, LAC has values of 0.17 to 0.2 cm-1 at an energy of 1 MeV, respectively. Because it has the largest atomic number and ρ, glass CuBi-12 has the highest LAC values [21]. The figure also demonstrates how the LAC varies linearly with Bi_2O_3 concentration at these chosen energies. This could also be explained by the fact that the glass combinations contain a range of metals (like Bi_2O_3) and non-metals (like PbO, B_2O_3, SiO_2 and CuO), as mentioned earlier. In the same perspective, as the amount of Bi^{3+} ions in the test glasses increases, so do the other dependent metrics including MFP, HVL, and RPE. CuBi-12 glass was seen to have good values for MAC, MFP, HVL, and RPE; CuBi-0, CuBi-3, CuBi-5, CuBi-8, and CuBi-12 glasses will also be beneficial as shielding glasses [22]. Overall, the concentration of Bi_2O_3 and the thickness of the glasses are the only factors that affect the radiation protection efficiency and shielding phenomena of the test glasses.

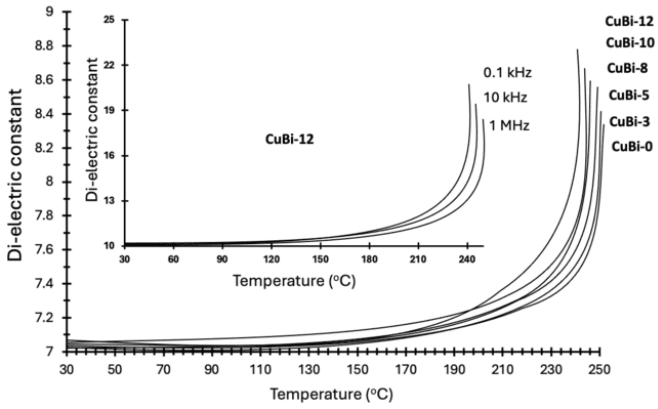

Fig 8. The variation in dielectric constant of 25 PbO + 15 B_2O_3 + 0.1 CuO + (59.9-x) SiO_2 :x Bi_2O_3 glasses with temperature. Inset shows the variation of dielectric constant of glass Cu Bi-12 with temperature at different frequencies

At 1 kHz, 10 kHz, and 100 kHz frequencies, as well as in the temperature range of 30 °C to 250 °C, the dielectric properties of the 25 PbO + 15 B_2O_3 + 0.1 CuO + (59.9-x) SiO_2 :x Bi_2O_3 glasses are measured. Wherein the temperature area of relaxation, activation energy conduction, ac conductivity, dielectric constant, and dielectric loss have all been assessed. The CuBi-12 glass was found to yield the best results. The change in dielectric constant with temperature is shown in Figure 8. The inset of the same image illustrates how the dielectric constant of CuBi-12 glass varies for frequency ranges of 1 kHz, 10 kHz, and 100 kHz. Figure 9 illustrates how di-electric loss changes with temperature. The variation in the dielectric loss of the CuBi-12 glass at 1 kHz, 10 kHz, and 100 kHz frequency ranges is reported in the inset of the same figure. Figure 10 illustrates how AC conductivity changes in response to an inverse temperature variation. The change in A.E. with increasing concentration of Bi_2O_3 is reported in the inset of the same figure. The dielectric constant, dielectric loss, ac conductivity, temperature zone of relaxation, and activation energy conduction with temperature and frequency all vary as the concentration of Bi_2O_3 grows due to differences in space charge polarization. polarization, which causes the variations in the values of dielectric constant, dielectric loss, ac conductivity, temperature region of relaxation, and activation energy conduction with temperature and frequency.

Some of the charge carriers in the glass network that travel across short atomic distances at lower frequencies trap the charge carriers inside the material's borders, resulting in space charge polarization. Due to this movement, the local field gets distorted, which increases the capacitance and eventually the dielectric constant [23]. At concentrations up to 12 mol%, Bi_2O_3 improves the space charge polarization, dielectric constant, loss tangent, and AC conductivity of the host glasses. Furthermore, a trend

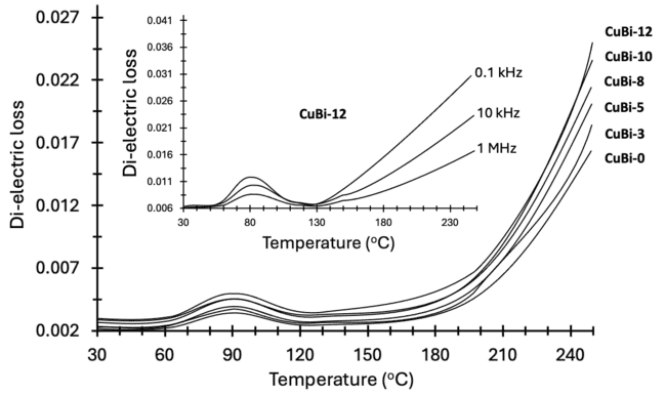

Fig 9. The variation of dielectric loss of 25 PbO + 15 B_2O_3 + 0.1 CuO + (59.9-x) SiO_2 :x Bi_2O_3 glasses with temperature. Inset shows the variation of dielectric loss with temperature at different frequencies of glass CuBi-12

of reversal in the Bi_2O_3 concentration is noted at 12 mol%. The relaxation time change exhibits compositional dependence as the concentration of Bi_2O_3 increases. The cross-linking of Bi^{3+} tetrahedral ions reduces as the concentration of Bi_2O_3 in the host glass exceeds 12 mol%. This reduces the generation of polaron-lattice ion couples, improving the dielectric constant, loss tangent, and ac conductivity for dipoles. From the same perspective, the glasses' activation energy increases over 12 mol% of the Bi_2O_3 concentration. At a specific frequency, space charge polarization is one of several polarization mechanisms in materials that causes the dielectric constant and AC conductivity to increase with temperature.

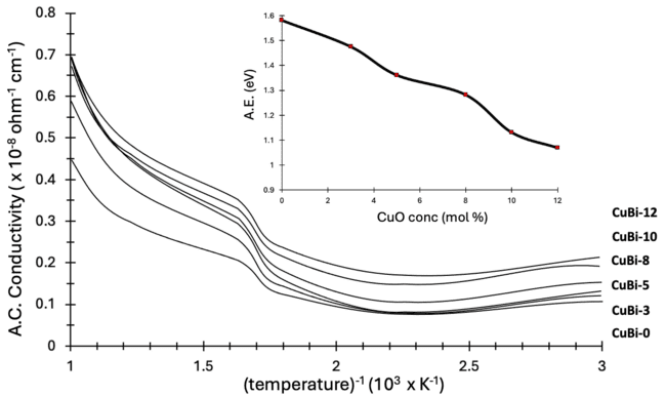

Fig 10. Variation of AC Conductivity of 25 PbO + 15 B_2O_3 + 0.1 CuO + (59.9-x) SiO_2 :x Bi_2O_3 glasses with 1/T. Inset shows the variation of activation energy with concentration of Bi_2O_3

Table 8. Summary on dielectric properties of 25 PbO + 15 B_2O_3 + 0.1 CuO + (59.9-x) SiO_2 :x Bi_2O_3 glasses

Glass	CuBi-0	CuBi-3	CuBi-5	CuBi-8	CuBi-10	CuBi-12
Di electric constant at 250°C,1 kHz	8.94	8.71	8.62	8.44	8.34	8.21
Di electric loss at 250°C, 1KHz	0.016	0.019	0.021	0.023	0.024	0.025
Ac Conductivity (ohm^{-1} cm^{-1})(x 10^{-8})	5.31	5.71	6.13	6.72	7.13	7.45
Temp region ofrelaxation(°C)	67-94	66-96	62-102	61-105	63-109	61-115
A.E forconduction(eV)	1.51	1.493	1.355	1.291	1.195	1.102

Changing ions (octahedrally positioned copper and borate ions mixed with Pb^{2+} ions) will cause bonding problems in the glass network. As a result, charge carriers can migrate more easily through these imperfections, which initiates space

charge polarization. The dielectric parameters and activation energy exhibit a positive correlation with progressive growth in concentration until reaching 12 mol% at any frequency and temperature. This suggests that the expanding quantities of octahedral Cu^{2+} ions functioning as modifiers contribute to an elevation in space charge polarization. An increase in the concentration of Bi_2O_3 beyond 12 mol% leads to an expansion of tetrahedral Cu^{2+} ions via glass forming connections with other elements of the tetrahedral glass network. This expansion ultimately results in a reduction in the space charge polarization. At lower frequencies, the QMT model deduces that the AC conductivity is determined by the density states of defects at the Fermi level $N(E_f)$. An increase in the quantity of CuO (up to 12 mol%) is observed to cause an increase in AC conductivity. This suggests that there are more free charge carriers available for conduction in the glass network or localized defect energy levels. However, above 12 mol% CuO, a reversal in conductivity is observed. As modifications, Cu^{2+} ions entering octahedral positions in the glass network will increase by up to 12 mol% of CuO the concentration of dangling bonds formed by lead ions and Cu^{2+} ions with different cations in the current glass samples[24]. The atomic radius of Cu^{2+} ions, tri-valent oxidation state of Cu^{2+} ions, density of the glasses, intermolecular force between the Cu^{2+} ions to Bi^{3+}, Pb^{2+}, $Si^{4+}$and B^{3+} ions, number of non-bridging oxygen's with in the glasses, and octahedral tendency of Cu^{2+} ions with in the glasses, is the main reason for enhanced properties of the structural, optical, radiation shielding and dielectric properties of present glasses. The specific results such as thermal stability (0.702), optical band gap (1.5 eV), radiation protection ability (~ 22%) and dielectric constant (~8.21) of present glasses are noticed to be great and comparable with previous literature (cited reference 13, 19, 21 and 23) are suggestable as thermally stable, optically active, radiation shielding dielectric glass resource.

4 Conclusion

The following conclusions are derived from the findings of the radiation shielding, optical, structural, and dielectric examinations of 25 PbO + 15 B_2O_3 + 0.1 CuO + (59.9-x) SiO_2 : x Bi_2O_3 glasses: Studies on glasses using XRD and SEM show glassy behavior. The chemical composition with atomic weight percentage is indicated by the EDX analysis. Physical parameters including density (~ 5.37 gm/cm^3) and molar volume (~ 30.46 cm^3 mol^{-1}) were determined to be optimal for the CuBi-12 glass. Similarly, the CrBi-12 glass was discovered to have the greatest values of GTT (about 594 °C) and thermal stabilities (about 0.702) evolutions in the DTA examinations of glasses. The evaluation of structural alterations in the glass network brought about by compositional variations is provided by the FT-IR and Raman investigations. Due to an increase in the modifying activity of octahedral Bi^{3+} ions, these spectral investigations showed a rising degree of disorder with a rise in Bi_2O_3 concentration in glass series up to 12 mol%. At very low levels of concentration, the optical band gap (1.5 eV) values are also solely dependent on the concentration of Bi_2O_3, according to the optical absorption experiments. Up to 12 mol% of the Bi_2O_3 concentration, the majority of the Cu^{2+} ions are arranged in octahedral orientations. Radiation shielding characteristics such as MAC (~ 41.04 cm^2/g) and RPE (~ 22%) show that the shielding behavior is solely dependent on Bi^{3+} ions. The range of the glasses' dielectric constant (~8.21), dielectric loss (~0.025), ac conductivity (~ 7.45 x 10^{-8} ohm^{-1} cm^{-1}) and A.E. (~ 1.102 eV) values are revealed by their dielectric characteristics. These findings further demonstrate that the glasses' dielectric behavior is solely dependent on the presence of Bi^{3+} ions. Overall, the created 25 PbO + 15 B_2O_3 + 0.1 CuO + (59.9-x) SiO_2 :x Bi_2O_3 glasses are useful resources that are dielectric, mechanically hard, and effectively shield radiation.

5 Author's contribution statement

Mr. Madabushanam Gopi Krishna: Methodology, characterization, results, report drafting.
Dr. Ravi Kumar Guntu: Methodology, analysis, and report correction.
Dr. Md Shareefuddin: suggestions and report corrections.
Dr. NV Prasad: Supervision, suggestions, and report corrections.

6 Acknowledgements

The authors thank to the management of Sreenidhi Institute of Science and Technology, for their needful help and moral support during overall completion of the investigation.

References

1) Chavan VK, Sreenivasulu M, Rao BRV. Optical applications of copper doped lithium phosphate glasses. *Optik*. 2020;221:165291. Available from: https://doi.org/10.1016/j.ijleo.2020.165291.
2) Tsaturyan AA, Cherkasova SO, Budnyk AP. Theoretical and experimental characterization of Cu-doped amorphous silicate glass. *Journal of Molecular Structure*. 2020;1205:127629. Available from: https://doi.org/10.1016/j.molstruc.2019.127629.

3) Ramadan RM, Hammad AH, Wassel AR. Impact of copper oxide on the structural, optical, and dielectric properties of sodium borophosphateglass. *Journal of Non-Crystalline Solids*. 2021;568:120961. Available from: https://doi.org/10.1016/j.jnoncrysol.2021.120961.
4) Zagrai M, Macavei GS, Popa A, Barbu-Tudoran L, Gavrea RC, Mereu AR, et al. Structural, thermal and physical properties of cesium doped molybdenum-copper-lead glass. *Journal of Non-Crystalline Solids*. 2023;619:122577. Available from: https://doi.org/10.1016/j.jnoncrysol.2023.122577.
5) Malekan M, Rashidi R, Shabestari SG, and JE. Thermodynamic and kinetic interpretation of the glass-forming ability of Y-containing Cu-Zr-Al bulk metallic glasses. *Journal of Non-Crystalline Solids*. 2022;576:121266. Available from: https://doi.org/10.1016/j.jnoncrysol.2021.121266.
6) Padlyak BV, Kindrat II, Kulyk YO, Hordieiev YS, Goleus VI, Lisiecki R. Spectroscopy and photoluminescence of complex lead-silicate glass doped with copper. *Materials Research Bulletin*. 2023;158:112071. Available from: https://doi.org/10.1016/j.materresbull.2022.112071.
7) Nazrin SN, Sharma A, Muhammad S, Alghamdi NA, Wageh S. Mechanical and radiation shielding properties of CuO doped TeO2–B2O3 glass system. *Radiation Physics and Chemistry*. 2022;198:110222. Available from: https://doi.org/10.1016/j.radphyschem.2022.110222.
8) Ouis MA, Marzouk MA. Comparative optical, FTIR and photoluminescence spectral analysis of copper ions in BaO–B2O3, SrO– B2O3 or Bi2O3– B2O3 glasses and impact of gamma irradiation. *Journal of Luminescence*. 2020;223:117242. Available from: https://doi.org/10.1016/j.jlumin.2020.117242.
9) Hussein EMA, Marzouk MA. Modeling and optical characterization of γ-irradiated Cu2+ Doped borate glasses as bandpass optical filters. *Journal of Physics and Chemistry of Solids*. 2023;181:111508. Available from: https://doi.org/10.1016/j.jpcs.2023.111508.
10) Abdelghany AM, Behairy A. Optical parameters, antibacterial characteristics and structure correlation of copper ions in cadmium borate glasses. *Journal of Materials Research and Technology*. 2020;9(5):10491–10497. Available from: https://doi.org/10.1016/j.jmrt.2020.07.057.
11) Mansour SF, Wageh S, Alotaibi MF, Abdo MA, Sadeq MS. Impact of bismuth oxide on the structure, optical features and ligand field parameters of borosilicate glasses doped with nickel oxide. *Ceramics International*. 2021;47(15):21443–21449. Available from: https://doi.org/10.1016/j.ceramint.2021.04.154.
12) Gomaa HM, Abul-Magd AA, Abu-Khadra AS, Yahia IS, and HYZ. Structural, and optical characterizations of Cu/Fe@Na2B4O7 oxide glass: For shielding and optical applications. *Optik*. 2022;261:169170. Available from: https://doi.org/10.1016/j.ijleo.2022.169170.
13) Zhang C, Cao Y, Shi J, Lu S, Gao E, Zhang M. Construction of copper-based core-shell composite for efficient removal of xanthate from wastewater. *Journal of Environmental Chemical Engineering*. 2023;11(6):111347. Available from: https://doi.org/10.1016/j.jece.2023.111347.
14) Ashok J, Kostrzewa M, Ingram A, Venkatramaiah N, Reddy MS, Kumar VR, et al. Structural and dielectric features of silver doped sodium antimonate glass ceramics. *Journal of Alloys and Compounds*. 2019;791:278–295. Available from: https://doi.org/10.1016/j.jallcom.2019.03.228.
15) Jiménez JA, Sendova M, Mancini M. Thermal and spectroscopic characterization of copper and erbium containing aluminophosphate glass. *Spectrochimica Acta Part A: Molecular and Biomolecular Spectroscopy*. 2020;226:117546. Available from: https://doi.org/10.1016/j.saa.2019.117546.
16) Reema KB, Jagannatha N, Nagaraja KP, D'Souza D. Impact of copper doping on thermal, optical and electrical properties of strontium L(+) tartrate pentahydrate crystals. *Journal of Crystal Growth*. 2021;574:126321. Available from: https://doi.org/10.1016/j.jcrysgro.2021.126321.
17) Sekhar AV, Kityk AV, Jedryka J, Rakus P, Wojciechowski A, Reddy ASS, et al. Investigations on the influence CuO doping on elastic properties of Li2SO4–MgO–P2O5 glass system by means of acoustic wave propagation. *Solid State Communications*. 2021;330:114270. Available from: https://doi.org/10.1016/j.ssc.2021.114270.
18) Krishnamoorthy A, Sakthivel P, Devadoss I, Rajathi VMA. Role of Bi3+ ions on structural, optical, photoluminescence and electrical performance of Cd0.9-xZn0.1BixS QDs. *SN Applied Sciences*. 2021;3(7):1–12. Available from: https://doi.org/10.1007/s42452-021-04681-7.
19) Ramanujan CS, Alrowaili ZA, Sekhar KC, Alzahrani JS, Shareefuddin MD, Haritha L, et al. Synthesis and Optimization of Bi2O3-B2O3-Cr2O3 Glass System for Structural, Optical, and Radiation Shielding Properties. *Journal of Electronic Materials*. 2023;52(10):6445–6459. Available from: https://doi.org/10.1007/s11664-023-10613-5.
20) Aloraini DA, Sayyed MI, Kumar A, Yasmin S, Almuqrin AH, Tishkevich DI, et al. Studies of physical, optical, and radiation shielding properties of Bi2O3-TeO2-MgO-Na2O-B2O3 glass system. *Optik*. 2022;268:169680. Available from: https://doi.org/10.1016/j.ijleo.2022.169680.
21) Shaaban SM, Alsaif NAM, Al-Ghamdi H, Khattari ZY, Rammah YS, El-Refaey AM, et al. Influence of Copper Ions on the Structural, Mechanical, Radiation Shielding and Dielectric Properties of Borate Zinc-Fluoride Glasses. *Journal of Electronic Materials*. 2023;52(9):6269–6276. Available from: https://doi.org/10.1007/s11664-023-10564-x.
22) Aloraini DA, Almuqrin AH, Saeed A. Impact of Bi3+, Ba2+, and Pb2+ ions on the structural, thermal, mechanical, optical, and gamma ray shielding performance of borosilicate glass. *Optical and Quantum Electronics*. 2024;56(1). Available from: https://doi.org/10.1007/s11082-023-05688-7.
23) Kayani ZN, Aslam H. Investigation of structural, optical, antibacterial, and dielectric properties of V-doped copper oxide thin films: Comparison with undoped copper oxide thin films. *Advanced Powder Technology*. 2021;32(7):2345–2358. Available from: https://doi.org/10.1016/j.apt.2021.05.026.
24) Shang Y, Wang M, Li E, Zhong C, Qin T. Enhancing thermal and dielectric properties of MgO–Al2O3–SiO2–B2O3 glass-ceramics through CuO doping. *Ceramics International*. 2023;49(19):32078–32085. Available from: https://doi.org/10.1016/j.ceramint.2023.07.175.